MNE 14 (2022) 100116

Contents lists available at ScienceDirect

Micro and Nano Engineering

journal homepage: www.sciencedirect.com/journal/micro-and-nano-engineering

Infrared polarimetry: Anisotropy of polymer nanofibers

Karsten Hinrichs [a,*], Brianna Blevins [c,d], Andreas Furchner [b], Nataraja Sekhar Yadavalli [c,d], Sergiy Minko [c,d,e]

[a] Leibniz-Institut für Analytische Wissenschaften – ISAS – e.V., Schwarzschildstraße 8, 12489 Berlin, Germany
[b] Helmholtz-Zentrum Berlin für Materialen und Energie, Division Energy and Information (CatLab Project), Schwarzschildstraße 8, 12489 Berlin, Germany
[c] Nanostructured Materials Laboratory, The University of Georgia, Athens, GA 30602, United States
[d] Department of Chemistry, The University of Georgia, Athens, Georgia 30602, United States
[e] Department of Textile, Fiber, and Polymer Sciences, The University of Georgia, Athens, Georgia 30602, United States

ARTICLE INFO

Keywords:
IR multi-scale metrology
Nanofiber
Polycaprolactone (PCL)
Touch-spinning
AFM-IR
Anisotropy
Ellipsometry

ABSTRACT

We present a straightforward and easily interpretable multi-scale infrared (IR) spectroscopic characterization of anisotropy and arrangement of polymer nanofibers. Direct spectral interpretation of fiber bundles and single fibers with respect to their anisotropic properties is possible by applying non-invasive IR polarimetry at defined polarization states with spatial resolutions from the macroscale (a few mm) down to the nanoscale (a few 10 nm). A vivid relation is shown to exist between vibrational bands in s-polarized reflection and absorption-associated photothermal spectra measured by the AFM-IR technique. Such a relation is a prerequisite for detailed discussions of IR spectra with respect to complex fiber structures and materials.

1. Introduction

Polymer nanofibers are of high technological relevance in optoelectronic [1], bio-related and medical research and technology fields [2–4], for example, as building blocks for fibrous scaffolds in neural tissue applications [3,4]. Functionalization, anisotropy, and ordering are key properties of fiber samples that require reliable and sensitive characterization procedures. In this work, we focus on a combined macroscale and nanoscale infrared polarimetric characterization for the direct interpretation of the anisotropic properties of touch-spun polycaprolactone (PCL) nanofibers. The recently developed touch-spinning method was used to produce nanofibers with scalable size in a simple and reproducible manner from polymer solutions [3,4]. The resulting aligned nanofiber scaffolds exhibit defined mechanical and optical properties, as well as homogeneous morphology on the studied length scales.

Few nanoscale IR studies of bare and functionalized fibers have been performed in the literature so far [6–10]. A comparison of nanoscale IR spectra of single fibers with polarized IR spectra of multiple aligned fibers was presented elsewhere [5,6]. Specific vibrational bands were discussed on a qualitative level [6]. In contrast, a quantitative in-depth interpretation of spectra–structure relations for anisotropic and heterogeneous sample materials typically requires advanced optical interpretations involving analytical and/or numerical optical calculations [11–15]. However, a model-free approach would often be preferable for assessment of the sample properties. It is therefore imperative to understand whether, and to which extent, it is possible to derive information on molecular structure, chemical structure, and orientation of single and multiple nanofibers from direct inspection of polarization-dependent AFM-IR spectra.

Here we present a multi-scale study of PCL nanofibers that provides comparable spectra for polarization-dependent AFM-IR of a single fiber and classical IR polarimetry of fiber bundles. Such a combined approach can deliver detailed information on fiber anisotropy and ordering without the need for optical simulations, thus laying the foundation for future nanoscale interpretation of complex nanofiber materials.

PCL is a semicrystalline polymer; the degree of crystallinity ranges from 20% to 80% depending on the fiber drawing conditions [4]. In this work, we study PCL nanofibers with an estimated crystallinity of 57% (as measured using XRD and DSC methods). In these samples, crystalline and amorphous phases contain aligned polymer chains that contribute to the fiber's anisotropy.

* Corresponding author.
E-mail address: karsten.hinrichs@isas.de (K. Hinrichs).

https://doi.org/10.1016/j.mne.2022.100116
Received 17 December 2021; Accepted 21 February 2022
Available online 26 February 2022

2. Experimental

2.1. Preparation

A set of fiber samples was prepared via the touch-spinning method (Fig. 1) on glass substrates and in a free-standing fashion on a wire collector from 8% polycaprolactone (PCL, M_n = 80,000 g/mol, Sigma-Aldrich) in chloroform (ACS grade, VWR Chemicals BDH). Details on touch-spinning can be found in Ref. [3].

2.2. IR polarimetric characterization

IR polarimetry of the samples was realized with polarization-dependent AFM-IR [11,12] and with classical IR polarimetry/ellipsometry in reflection [13,14]. A schematic presentation of these multi-scale polarimetric methods is shown in Fig. 2. A Mueller-matrix ellipsometer was used for complementary measurements of transmission spectra [16,17].

2.3. AFM-IR

For polarization-dependent AFM-IR measurements, a commercial NanoIR2-FS set-up (Anasys Instruments Corporation, BRUKER) with a polarizing unit and a pulsed mid-IR quantum cascade laser (QCL, MIRcat-QT, Daylight Solutions Inc.) in a top-down configuration was used. The QCL consists of four individual chips with emission starting at 900 cm^{-1}, 1127 cm^{-1}, 1419 cm^{-1} and 1544 cm^{-1}. Polarization-dependent sample spectra were referenced to the polarization-dependent background spectra of these four ranges. Measurements with a lateral resolution of about 30 nm were performed in contact mode using a gold-coated silicon AFM tip. Spectra were taken at 70° angle of incidence and 1 cm^{-1} spectral resolution. For further details see Ref. [11, 12].

2.4. IR polarimetry/ellipsometry

Polarization-dependent IR reflectance, amplitude (tan Ψ) and phase (Δ) ellipsometric spectra (see inset in Fig. 2) were measured at an incidence angle of 70° and at 4 cm^{-1} spectral resolution in a dry-air purged ellipsometer set-up with a photometric liquid-nitrogen-cooled mercury cadmium telluride (MCT) detector externally attached to an FTIR spectrometer (IFS 55 or Vertex 70, Bruker Optics, Ettlingen, Germany). Cross- and co-polarized transmittance spectra were obtained in a Mueller-matrix ellipsometer under azimuthal sample rotation (customized ELL14K mount, Thorlabs).

3. Results

3.1. Anisotropy of fiber scaffolds

Two types of anisotropy can influence the measured spectra of a fiber scaffold: Firstly, the anisotropy of the scaffold in dependence of the relative alignment of the single fibers within the probing spot; and secondly, the anisotropy of the individual fiber due to an average molecular orientation. For a well-aligned scaffold, closely related spectra would be expected for the fiber ensemble and the single fiber.

Fig. 3 shows s-polarized reflection spectra of the vertically and the horizontally aligned PCL fiber scaffold on glass. The observed absorption-like bands are consistent with Ref. [17], which discusses characteristic vibrations of PCL chains in spin-coated films on gold surfaces. Our data agree with the authors' orientation analysis, assuming an anisotropic alignment of the polymer chains within the fibers. All bands in Fig. 3, except for the ν(C=O) mode, exhibit a pronounced anisotropy, as identified by the significant changes in band amplitudes with in-plane sample rotation. The transition dipole moments (TDMs) of these vibrations are thus aligned predominantly along the direction of the polymer chains.

In contrast to s-polarized reflection spectra (and to normal-incidence

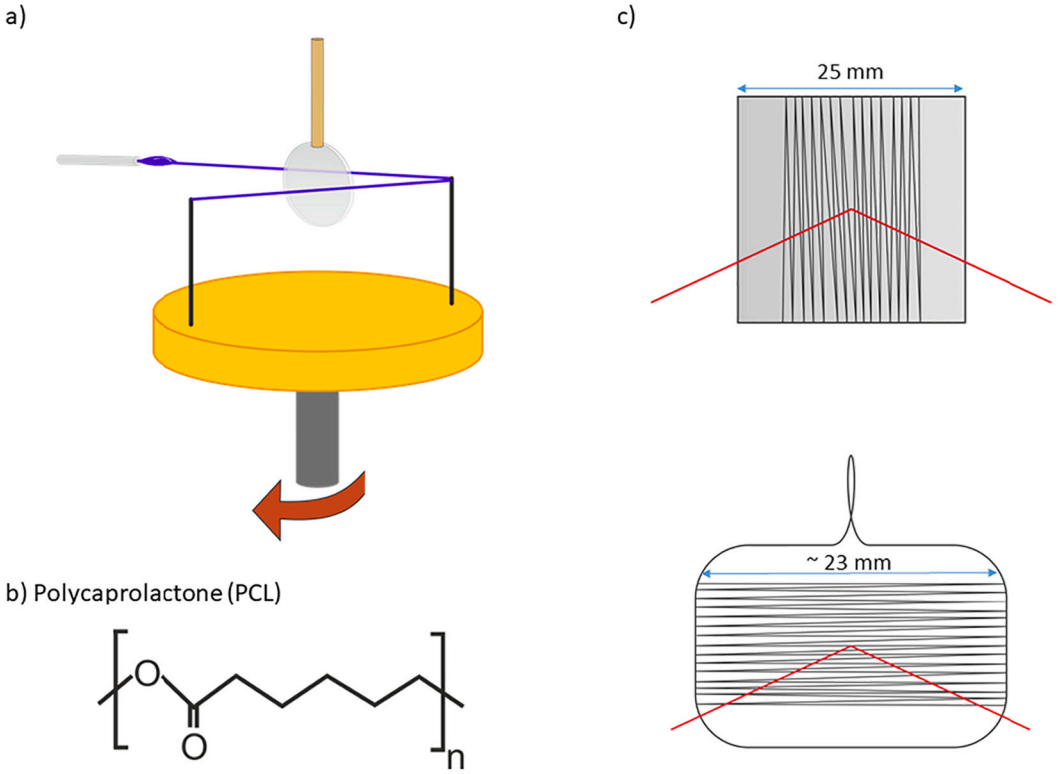

Fig. 1. a) Sketch of the touch-spinning method, in which a rotating disc holds two rods that collect a continuous fiber from a polymer droplet; b) Structure of polycaprolactone (PCL); c) Schematic figure of fiber scaffolds prepared around a square glass substrate and "free-standing" around a wire collector.

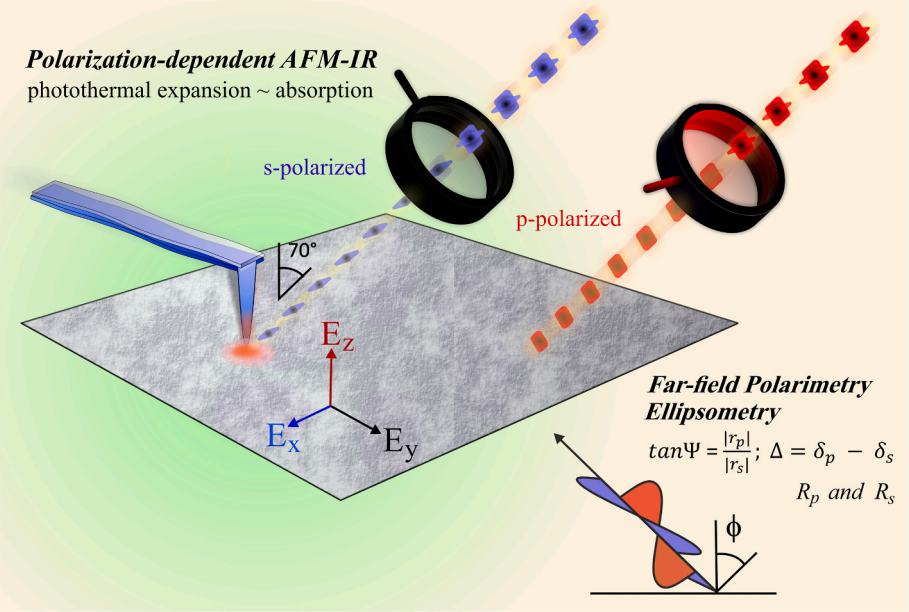

Fig. 2. Schematic presentation of 1) Polarization-dependent AFM-IR measuring the photothermal expansion (absorption) of the sample surface by an AFM tip upon polarized irradiation; and 2) Classical polarimetry/ellipsometry measuring ellipsometric parameters (tan Ψ and Δ) and polarization-dependent reflectances (R) and transmittances (T) under an incidence angle ϕ of choice. s-polarization is in x-direction perpendicular to the y–z incidence plane.

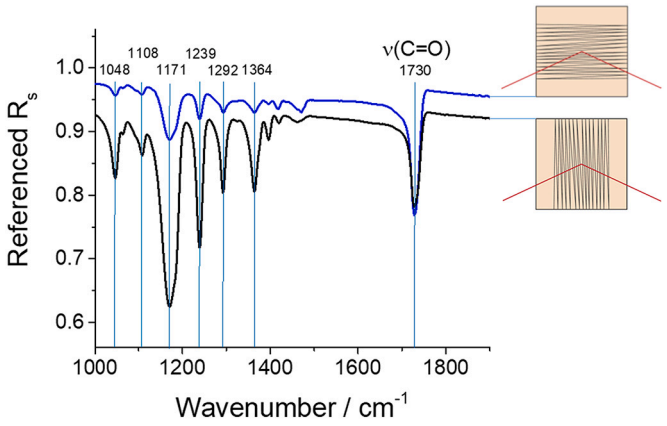

Fig. 3. s-polarized reflection spectra (referenced to the s-polarized reflection of the bare glass surface) for differently aligned PCL scaffold on a glass substrate. Positions of peak maxima are indicated.

transmission spectra), the vibrational features in unpolarized and p-polarized reflection spectra, as well as in ellipsometric tan Ψ and Δ spectra, do not display simple absorption-like bands. Field components of the probing radiation in direction perpendicular to the surface are causing altered band shapes in spectra of anisotropic thin films and fiber materials. Interestingly, the resulting characteristic band shapes, for example in tan Ψ and Δ, are correlated with the average orientation of the related TDMs, as previously demonstrated by ordering- and orientation-dependent optical simulations for various other thin film samples [18–21].

Characteristic band shapes, and changes thereof, are exemplarily identified in Fig. 4, showing Kramers–Kronig consistent tan Ψ and Δ spectra of the PCL nanofiber scaffold. The marked bands differ in shape and amplitude upon changing of the fiber orientation. A detailed analysis of this finding is beyond the scope of this article and would require in-depth optical simulations.

Next, we performed cross- and co-polarized transmission measurements (T_{ps} and T_{ss}) of the free-standing wire-collector under 2π azimuthal rotation (see Fig. 5). The resulting spectra enable a more detailed inspection of the fiber scaffold's anisotropy related to the direction of average TDMs of the respective vibrations. While T_{ss} naturally captures all vibrational contributions along the polarization axes, T_{ps} is only sensitive to, and non-zero for, anisotropic contributions.

The two most intense characteristic vibrations and their specific TDMs are marked in Fig. 5, namely the C=O stretching mode around 1730 cm^{-1} and the asymmetric C–O–C stretching mode around 1239 cm^{-1} (assignment according to Ref. [22]). The presented cross-polarized T_{ps} spectra show significant contributions only between 1000 cm^{-1} and 1440 cm^{-1}, and for sample rotations around 45°, 135°, 225° and 315°. At rotations around 0°, 90°, 180° and 270°, T_{ps} approaches zero, suggesting that the average TDMs are either parallel or perpendicular to the optical axes of the scaffold, i. e., to the macroscopic fiber directions. Maximum band intensities in T_{ss} are observed around 90° and 270°. The TDMs of these bands are therefore distributed predominantly along the direction of the fibers, in accordance with the previously discussed reflection spectra. In contrast, no significant contribution of the ν(C=O)-related band is observed in T_{ps}, but an almost rotation-independent band is seen in T_{ss}, indicating an overall isotropic distribution of the ν(C=O)-related TDMs. This finding implies that the average orientation of C=O bonds within the PCL polymer chains is not simply perpendicular to the direction of the nanofiber, as would be expected for a single molecule.

Several horizontal stripes that are independent of vibrational absorption bands are seen in T_{ss}. Such baseline effects are assigned to a certain degree of macroscopic inhomogeneity of the scaffold, for example, to a slightly varying density of fibers on the mm scale.

3.2. Nanoscale AFM-IR

Finally, we employed AFM-IR to study individual fibers on the nanoscale. Fig. 6 compares representative s-polarized AFM-IR spectra of a single 460 nm thick fiber with macroscopic s-polarized reflection spectra of fiber bundles in a scaffold. Both the single fiber and the fiber scaffold were oriented at about 63° and − 27° (rotated by −90°) with respect to the plane of incidence. Overall agreement between the two sets of spectra is observed regarding band frequencies and shapes. Small deviations in relative band amplitudes are present but could be explained by optical effects and by macroscopic averaging. While AFM-

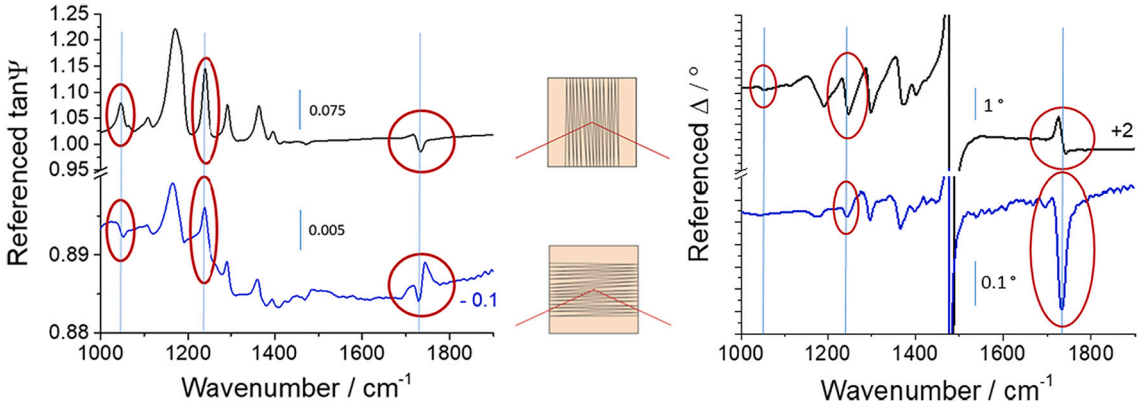

Fig. 4. Ellipsometric tan Ψ (left) and Δ spectra (right) (referenced to corresponding tan Ψ and Δ spectra of the bare glass surface) for the horizontally and vertically aligned scaffold on a glass substrate. Characteristic band shape changes are marked. For better comparison, the bottom tan Ψ and Δ spectra are zoomed-in by a factor of 15 and 10, respectively.

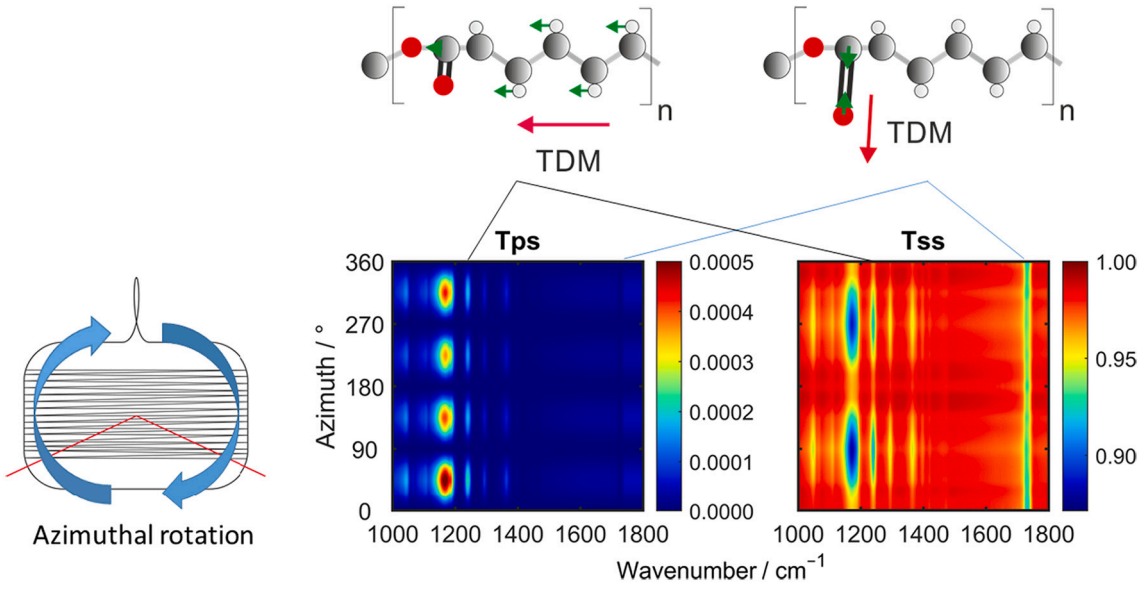

Fig. 5. Transmittance measured with crossed polarizers (T_{ps}) and parallel polarizers (T_{ss}) for azimuthal rotation of a free-standing fiber scaffold on a wire collector. Two characteristic vibrations, the asymmetric C–O–C stretching and C=O stretching modes, and their transition dipole moments (TDMs) are marked. Green arrows indicate the displacements of the single atoms. (For interpretation of the references to colour in this figure legend, the reader is referred to the web version of this article.)

IR is probing a single well-oriented fiber, classical polarimetry is sensitive only to the average orientation angle of the measured set of fibers within the macroscopic scaffold. Compared to the s-polarized spectra of the 0° and 90° oriented fibers in Fig. 3, the 63° and − 27° oriented fibers in Fig. 6 show remarkably similar intensities of the absorption band between 1000 cm^{-1} and 1440 cm^{-1}. These band amplitudes exhibit a cosine dependence on the azimuth angle, explaining why the relative spectral band intensity changes from 0° towards −27° are stronger than those from 90° to 63°.

In conclusion, the presented nanoscale PCL absorption data prove to be comparable with macroscale s-polarized reflection spectra for this kind of polymer material. Future work will thus aim at analyzing and using the nanoscale fiber orientation for understanding in more detail the macroscopic averaged optical response of the scaffold. This will open the door for multi-scale investigations of more complex, potentially less well-oriented, fiber materials, or even fiber scaffolds with crisscross fiber orientations.

4. Conclusions

By comparing the vibrational bands in s-polarized reflection spectra with those in s-polarized photothermal AFM-IR spectra, we ensure that only related in-plane absorption properties are detected. A good correlation between the respective results for a single fiber and a set of oriented fibers was found. Azimuthal transmission measurements of fiber scaffolds can also probe the in-plane vibrational properties and are well-suited for direct discrimination of anisotropically and isotropically oriented transition dipole moments. Cross-polarization transmission measurements confirm these results and may serve as a quick identifier of anisotropies.

Author contributions

Karsten Hinrichs: Conceptualization, Methodology of IR measurements, IR Investigation, Writing – original draft; Visualization. Brianna Blevins: Resources, Sample Preparation. Andreas Furchner: Methodology of IR measurements, IR Investigation, Writing – review & editing,

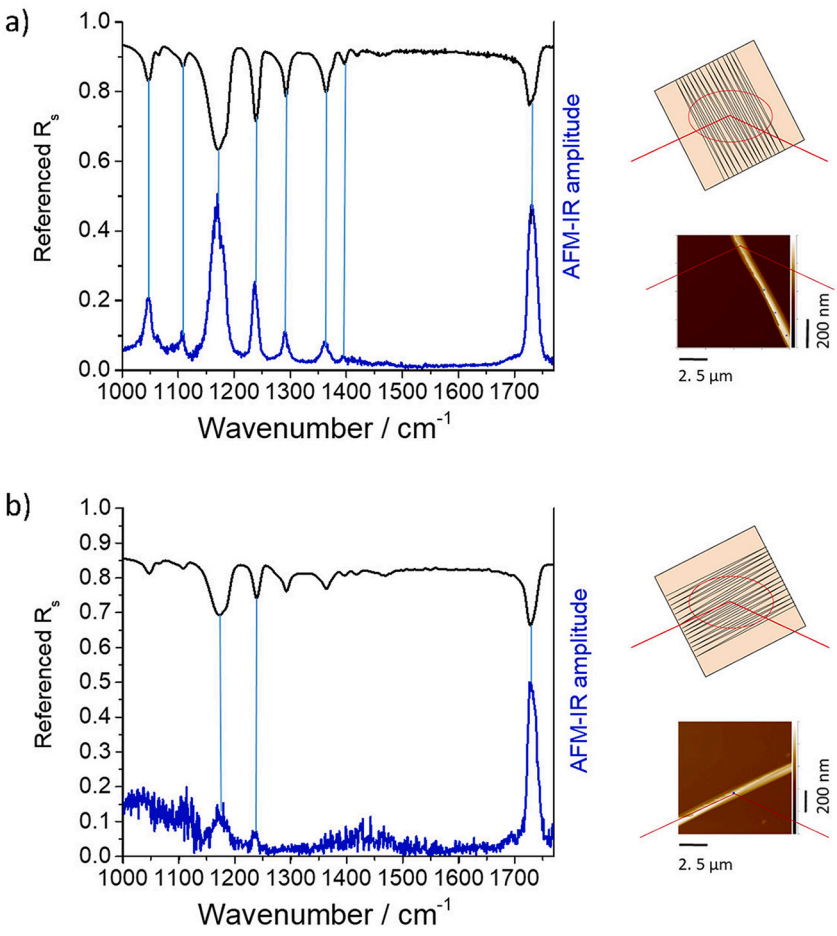

Fig. 6. Left: Azimuthal rotation of about a) 63° and b) –27°, each comparing normalized s-polarized AFM-IR spectra (blue / bottom) of a single fiber with s-polarized reflection spectra (black / top) of a fiber scaffold. Right: Corresponding schematics of the fiber scaffold with the elliptical probing spot indicated (thin red line), and AFM image of the single about 460 nm thick fiber. (For interpretation of the references to colour in this figure legend, the reader is referred to the web version of this article.)

Visualization. Nataraja Sekhar Yadavalli: Assembling of fiber touch-spinning set-up. Sergiy Minko: Resources, Methodology of fiber preparation, Writing – review & editing.

Declaration of Competing Interest

The authors declare that they have no known competing financial interests or personal relationships that could have appeared to influence the work reported in this paper.

Acknowledgements

We acknowledge financial support by the European Union through EFRE 1.8/13, as well as financial support by the Ministerium für Kultur und Wissenschaft des Landes Nordrhein-Westfalen, Die Regierende Bürgermeisterin von Berlin - Senatsverwaltung für Wissenschaft, Gesundheit, Pflege und Gleichstellung, and the Bundesministerium für Bildung und Forschung. The authors acknowledge support from the Federal Ministry of Education and Research in the framework of the project Catlab (03EW0015A).

References

[1] P. Wang, Y. Wang, L. Tong, Functionalized polymer nanofibers: a versatile platform for manipulating light at the nanoscale, Light Sci. Appl. 2 (2013), e102, https://doi.org/10.1038/lsa.2013.58.

[2] K.C. Gupta, A. Haider, I.-K. Kang Choi, Nanofibrous scaffolds in biomedical applications, Biomater Res. 18 (2014) 5, https://doi.org/10.1186/2055-7124-18-5.

[3] S.-J. Lee, D. Asheghali, B. Blevins, R. Timsina, T. Esworthy, X. Zhou, H. Cui, S. Y. Hann, X. Qiu, A. Tokarev, S. Minko, L.G. Zhang, Touch-spun nanofibers for nerve regeneration, ACS Appl. Mater. Interfaces 12 (2020) 2067–2075, https://doi.org/10.1021/acsami.9b18614.

[4] D. Asheghali, S.J. Lee, A. Furchner, A. Gruzd, S. Larson, A. Tokarev, S. Stake, X. Zhou, H.K. Inrichs, L.G. Zhang, S. Minko, Enhanced neuronal differentiation of neural stem cells with mechanically enhanced touch-spun nanofibrous scaffolds, Nanomedicine 24 (2020), 102152, https://doi.org/10.1016/j.nano.2020.102152.

[5] A. Dazzi, C.B. Prater, Q. Hu, D.B. Chase, J.F. Rabolt, C. Marcott, AFM–IR: combining atomic force microscopy and infrared spectroscopy for nanoscale chemical characterization, Appl. Spectrosc. 66 (2012) 1365–1384, https://doi.org/10.1366/12-06804.

[6] G. Bakir, B.E. Girouard, R. Wiens, S. Mastel, E. Dillon, M. Kansiz, K.M. Gough, Orientation matters: polarization dependent IR spectroscopy of collagen from intact tendon down to the single fibril level, Molecules 25 (2020) 4295, https://doi.org/10.3390/molecules25184295.

[7] Z. Wang, B. Sun, X. Lu, C. Wang, Z. Su, Molecular orientation in individual electrospun nanofibers studied by polarized AFM–IR, Macromolecules 52 (2019) 9639–9645, https://doi.org/10.1021/acs.macromol.9b01778.

[8] E. Suzuki, A quantitative study of the amide vibrations in the infra-red spectrum of silk fibroin, Spectrochim. Acta A: Mol. Spectrosc. 23 (8) (1967) 2303–2308, https://doi.org/10.1016/0584-8539(67)80123-5.

[9] T. Igarashi, M. Hoshi, K. Nakamura, T. Kaharu, K.-I. Murata, Direct observation of bound water on cotton surfaces by atomic force microscopy and atomic force microscopy–infrared spectroscopy, J. Phys. Chem. C 124 (2020) 4196–4201, https://doi.org/10.1021/acs.jpcc.0c00423.

[10] M. Ryu, R. Honda, A. Cernescu, A. Vailionis, A. Balčytis, J. Vongsvivut, L.-L. Li, D. P. Linklater, E.P. Ivanova, V. Mizeikis, M.J. Tobin, J. Morikawa, S. Juodkazis, Nanoscale optical and structural characterisation of silk, Beilstein J. Nanotechnol. 10 (2019) 922–929, https://doi.org/10.3762/bjnano.10.93.

[11] K. Hinrichs, T. Shaykhutdinov, Polarization-Dependent Atomic Force Microscopy–Infrared Spectroscopy (AFM-IR): Infrared Nanopolarimetric Analysis of Structure and Anisotropy of Thin Films and Surfaces, Appl. Spectrosc. 72 (2018) 817, https://doi.org/10.1177/0003702818763604.

[12] T. Shaykhutdinov, S.D. Pop, A. Furchner, K. Hinrichs, Supramolecular orientation in anisotropic assemblies by infrared Nanopolarimetry, ACS Macro Lett. 6 (2017) 598, https://doi.org/10.1021/acsmacrolett.7b00147.

[13] A. Röseler, E.-H. Korte, Infrared spectroscopic ellipsometry, in: J.M. Chalmers, P. R. Griffiths (Eds.), Handbook of vibrational spectroscopy vol. 62, Wiley, Chichester, 2002, https://doi.org/10.1002/0470027320.s2208.

[14] Ellipsometry of functional organic surfaces and films, in: K. Hinrichs, K.-J. Eichhorn (Eds.), Springer Series in Surface Sciences, 2nd ed., in: G. Ertl, H. Lüth, R. Car, M.A. Rocca, H.-J. Freund, S. Hasegawa (Eds.) vol. 52, Springer Nature, 2018. https://link.springer.com/book/10.1007/978-3-319-75895-4.
[15] M. Losurdo, K. Hingerl (Eds.), Ellipsometry at the Nanoscale, Springer Verlag Berlin Heidelberg, 2013.
[16] A. Furchner, C. Walder, M. Zellmeier, J. Rappich, K. Hinrichs, Broadband infrared Mueller-matrix Ellipsometry for studies of structured surfaces and thin films, Appl. Opt. 57 (2018) 7895–7904, https://doi.org/10.1364/AO.57.007895.
[17] A. Furchner, C. Kratz, W. Ogieglo, I. Pinnau, J. Rappich, K. Hinrichs, Ultrasensitive broadband infrared 4 × 4 Mueller-matrix ellipsometry for studies of depolarizing and anisotropic thin films, JVST B 38 (2020), 014003, https://doi.org/10.1116/1.5129800.
[18] K. Hinrichs, M. Levichkova, D. Wynands, K. Walzer, K.-J. Eichhorn, P. Bäuerle, K. Leo, M. Riede, Morphology and molecular orientation of ethyl-substituted dicyanovinyl-sexithiophene films for photovoltaic applications, Thin Solid Films 525 (2012) 97–105, https://doi.org/10.1016/j.tsf.2012.10.069.
[19] D.M. Rosu, J.C. Jones, J. Hsu, K.L. Kavanagh, D. Tsankov, U. Schade, N. Esser, K. Hinrichs, Langmuir 25 (2009) 919–923, https://doi.org/10.1021/la8026557.
[20] K. Roodenko, J. Rappich, F. Yang, X. Zhang, N. Esser, K. Hinrichs, Anisotropy in hydrogen-passivated and organically modified Nanoporous silicon surfaces studied by polarization dependent IR spectroscopy, Langmuir 25 (2009) 1445–1452, https://doi.org/10.1021/la802685m.
[21] K. Hinrichs, M. Gensch, N. Esser, Analysis of organic films and interfacial layers by infrared spectroscopic Ellipsometry, Appl. Spectr. 59 (2005) 272A–282A, https://doi.org/10.1366/000370205774783106.
[22] J.T. Elzein, M. Nasser-Eddine, C. Delaite, S. Bistac, P. Dumas, J. Colloid Interface Sci. 273 (2004) 381–387, https://doi.org/10.3390/molecules2518429.